

---

# Expansive Synthesis: Generating Large-Scale Datasets from Minimal Samples

---

**Vahid Jebraeeli**

Electrical Engineering Department  
North Carolina State University  
Raleigh, NC 27606  
vjebrae@ncsu.edu

**Bo Jiang**

Neuroscience Department  
Washington University  
St. Louis, MO 63130  
bo.j@wustl.edu

**Hamid Krim**

Electrical Engineering Department  
North Carolina State University  
Raleigh, NC 27606  
ahk@ncsu.edu

**Derya Cansever**

Electrical Engineering Department  
North Carolina State University  
Raleigh, NC 27606  
dhcansev@ncsu.edu

## Abstract

The challenge of limited availability of data for training in machine learning arises in many applications and the impact on performance and generalization is serious. Traditional data augmentation methods aim to enhance training with a moderately sufficient data set. Generative models like Generative Adversarial Networks (GANs) often face problematic convergence when generating significant and diverse data samples. Diffusion models, though effective, still struggle with high computational cost and long training times. This paper introduces an innovative Expansive Synthesis model that generates large-scale, high-fidelity datasets from minimal samples. The proposed approach exploits expander graph mappings (mathematically known as dimension expansion) and feature interpolation to synthesize expanded datasets while preserving the intrinsic data distribution and the feature structural relationships. The rationale of the model is rooted in the non-linear property of neural networks' latent space and in its capture by a Koopman operator to subsequently yield a linear space of features to facilitate the construction of larger and enriched consistent datasets starting with a much smaller dataset. This process is optimized by an autoencoder architecture enhanced with self-attention layers and further refined for distributional consistency by optimal transport. We validate our Expansive Synthesis by training classifiers on the generated datasets and by comparing their performance to classifiers trained on larger, original datasets. Experimental results demonstrate that classifiers trained on synthesized data achieve performance metrics on par with those trained on full-scale datasets, showcasing the model's potential to effectively augment training data. This work represents a significant advancement in data generation, offering a robust solution to data scarcity and paving the way for enhanced data availability in machine learning applications.<sup>1</sup>

## 1 Introduction

In modern machine learning, it is important, and often critical to generate large training datasets from a small number of samples. The data scarcity in many applications (e.g., biomedical, aerial,

---

<sup>1</sup>Thanks to the generous support of ARO grant W911NF-23-2-0041.

etc.), often limits acceptable performance and generalizability. This demand is expected to increase with the adoption of AI/ML methodology across diverse fields, and the urgency of the issue becomes more pressing. Existing data augmentation techniques, as later discussed, and Generative Adversarial Networks (GANs) fall short on account of acceptable diversity and even stability in the latter case. Our proposed "Expansive Synthesis" emerges as a pioneering solution to this challenge, offering an intuitively appealing and mathematically sound framework to synthesize extensive datasets from limited data input. This approach mitigates the data sufficiency issue as well as the richness quality to obtain efficient and effective training data. This is fundamentally based on the so-called "dimension expansion" [Forbes and Guruswami, 2014] and its equivalent formulation of "expansion graphs" [Margulis, 1973] in graph theory, and on leveraging self-attention [Vaswani et al., 2017] and optimal transport [Villani, 2009] to ensure a good regularization of the synthesis.

Data augmentation in deep learning, consisting of geometric transformations and color space manipulations, include horizontal flipping, rotation, cropping, and adjusting color channels, to enhance the generalization capabilities of convolutional neural networks (CNNs). Other techniques, like Random Oversampling (ROS) and Synthetic Minority Over-sampling Technique (SMOTE) Chawla et al. [2002], addressed class imbalances by generating synthetic samples through interpolation of minority class instances, each with their own limitations such as overfitting/duplication and unrealistic distortion. GANs Goodfellow et al. [2014], have also further contributed to data augmentation. They have yielded high-quality synthetic data, with direct relevance data augmentation. Subsequent advancements such as Deep Convolutional GANs (DCGANs) by Radford et al. [2015], and CycleGANs by Zhu et al. [2017] further enhanced the resolution and realism of generated images, with Neural Style Transfer Gatys et al. [2015] adding a new artistic style dimension to image data augmentation and Fast Style Transfer [Johnson et al., 2016] adding other visual features. All these, however, still face instability issues during training, primarily on account of mode collapse, as well as on difficulty with diversity of samples. Meta-learning approaches, such as Neural Architecture Search (NAS) and AutoAugment [Cubuk et al., 2019], have refined data augmentation strategies by automating the search for optimal augmentation policies, at a complexity cost, still making them more appropriate for only smaller-scale projects.

Our work is inspired by the inherent capacity of neural networks to extrapolate from minimal data, a concept rooted in the expansive nature of latent space representations. Traditional data augmentation techniques falling short in scenarios with severely limited data, prompt the need for innovative solutions that can generate large-scale datasets while preserving the core characteristics of the original samples. The "Expansive Synthesis" model is conceived to address this challenge by transforming small datasets into expansive, high-fidelity datasets through advanced synthesis techniques. As noted, by leveraging regularization techniques (e.g., self-attention mechanism [Vaswani et al., 2017]), our approach builds on dimension expansion and its expander graph perspective [Forbes and Guruswami, 2014] to exploit extracted features for robust data synthesis with proper distribution to facilitate training learning models. This approach effectively reverses the flow of recent advances in data condensation techniques [Anonymous, 2024]. Specifically, we describe a framework where, as we further elaborate later, all extracted and attention-driven features define a Koopman space where nonlinear feature components are optimally chosen to be linearly combined for dimension expansion, all the while preserving the intrinsic distribution of the data by optimal transport. The paper flow proceeds as follows: Section 2 provides a background on Koopman Operator Theory and its application in deep learning [Koopman, 1931, Dey and Davis, 2023]. Section 3 details the Expansive Synthesis model, explaining its formulation, design, and its realizations as a coherent entity. Section 4 presents our experimental validation, demonstrating the model's effectiveness in generating expansive datasets and evaluating classifier performance on these datasets relative to traditional methods. The final section, 5, concludes the paper, summarizing key findings and outlining potential future directions.

## 2 Related Background

For clarity, we provide a brief overview of the theoretical tools which underpin our proposed algorithm development. To start, a Koopman operator Koopman [1931] offers a linear perspective on nonlinear dynamical systems. We specifically describe an estimation of a Koopman operator using deep learning techniques. We next discuss how to best preserve the distribution of data using Optimal Transport (OT) and highlight recent advancements.

## 2.1 Koopman Feature Space

Koopman operator theory offers a rich and elegant framework for analyzing nonlinear dynamical systems by transforming them into a linear context. Koopman first proposed a theory to facilitate the study of complex systems using linear operators on function spaces, regardless of the nonlinearity in the state space [Koopman, 1931] (see Appendix A for more detailed explanation and formal theorems). Building on this theory, recent contributions in deep learning have facilitated the approximation of the Koopman operator using neural networks, allowing for practical applications in a variety of complex systems. (See Appendix B for details).

## 2.2 Data Distribution Preservation

It is critical to preserve the distribution of a synthesized expanded dataset to safeguard its utility for further training (or other) purposes. To that end, OT is used for regularization, as illustrated in Fig. 6(b). Additional details will be discussed in the Methodology section as well as Appendix D.

## 3 Methodology

In pursuing our objective, we have:

**Claim:** *A near-optimal and feature consistent expansion  $X'$  of a dataset  $X$  can be achieved in a Koopman-data space using Expander Graph Mapping, with proper distribution and feature refinement regularizations.*

As depicted in Figure 1, this methodology is engineered to expand a minimal sample dataset  $X$  into the expanded yet informatively preservative set  $X'$ , crafted to retain the crucial attributes of the original dataset, exploiting the Koopman linear evolution of non-linear dynamics Koopman [1931]. The latent representation  $Y \in \mathbb{R}^{n \times d}$  is the result of  $\phi : \mathbb{R}^{n \times D} \rightarrow \mathbb{R}^{n \times d}$  with  $d < D$ , and is followed by a Multi-head Spatial Self-Attention Mechanism to capture the most discriminative data features and Expander Graph Mapping Dey and Davis [2023] to generate new diverse data-points by keeping the original distribution of original dataset controlled by Wasserstein distance and Covariance loss.

To pursue the dimension expansion of small but diverse data sets, we first define a functional space where a meaningful preservation of non-linear features characteristic of train data at hand. To that end, and as illustrated on the left-hand side of Fig. 6(b), we aim to glean a Koopman-like characterization of data across all classes of interest as defined above. Given any data sample as an aggregate of extracted features (possibly refined by an attention mechanism), it may be interpreted as a set of nodes structured as a graph. Applying an expander graph property on such a graph, will give rise to the expansive synthesis with a generative capability as further developed next.

### 3.1 Autoencoder:Koopman Feature Space

In the pre-training phase of our "Expansive Synthesis" project, a convolutional Autoencoder (AE) is employed, leveraging a substantial dataset  $X''$  that is analogous to the target smaller dataset  $X$ . This phase is critical as it equips the AE with a robust understanding of the general features present in a large dataset. The AE's architecture comprises multiple convolutional layers, each defined by weight parameters  $W_1, W_2, \dots, W_{cout}$ . These weights are meticulously optimized to capture and encode essential data characteristics Goodfellow et al. [2014], Krizhevsky et al. [2012].

The convolutional transformation for each layer is expressed as  $\text{conv}(x; W_i)$ , where  $W_i$  denotes the  $i$ th filter, and  $cout$  is the total number of output channels. The AE reduces the dimensionality of the dataset, encoding it into a compressed representation  $Y''$ , which retains the most significant features of the input data. The objective during pretraining is to minimize a reconstruction loss, ensuring that the AE learns a compact and informative representation of the dataset  $X''$ . This foundational pre-training is depicted in Figure 1 (a), where the similar dataset  $X''$  is encoded into  $Y''$  through the function  $\phi$ , and subsequently decoded back to its original space using  $\phi^{-1}$ .

In adapting the Koopman-Autoencoder to the smaller dataset  $X$ , we seek to optimize its pre-trained weights  $W$  to capture the specific characteristics of  $X$ . To that end, a model introduces scaling ( $\gamma$ ) and shifting ( $\beta$ ) parameters, which are dynamically optimized to aptly fine-tune the AE's performance on the smaller dataset. Computationally, the convolution operation during fine-tuning is defined as:

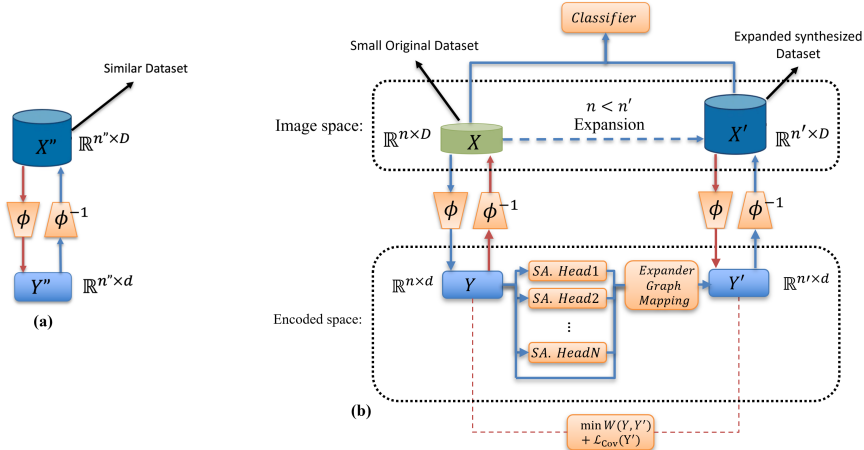


Figure 1: Overall architecture of Expansive Synthesis model. **(a)** Pretraining phase using a similar larger dataset  $X''$  to learn general features, which are encoded and decoded to produce  $Y''$ . **(b)** Fine-tuning phase on the smaller target dataset  $X$  to adapt the model’s weights, followed by the expansion of  $X$  to generate the synthesized dataset  $X'$  using expander graph mapping and self-attention mechanisms. The expanded dataset  $X'$  is then used to train a classifier.

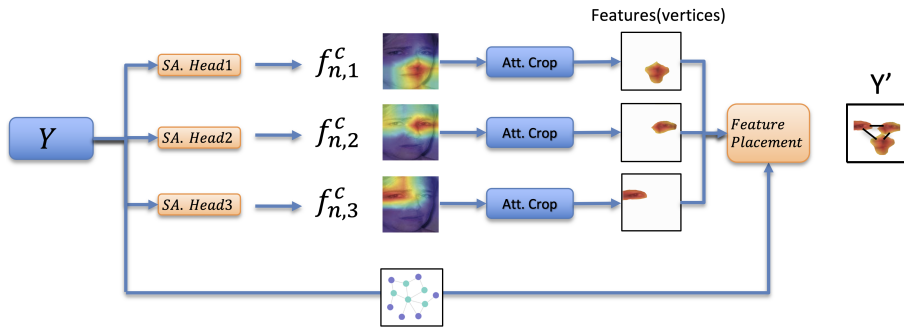


Figure 2: Architecture of Expander Graph Mapping

$$\text{conv}(x; W) \cdot \gamma + \beta = \text{conv}(x; \{\gamma_1 W_1 + \beta_1, \dots, \gamma_{\text{cout}} W_{\text{cout}} + \beta_{\text{cout}}\}) \quad (1)$$

Here,  $\gamma_i$  serves to adjust the activation strength of each filter, thereby controlling the sensitivity to input features He et al. [2016]. A higher  $\gamma_i$  enhances the filter’s response to specific features, while  $\beta_i$  modifies the activation threshold, making the neuron "more" or "less" prone to activation. These parameters are tailored for each filter, allowing for precise adaptation to the nuances of the smaller dataset  $X$ . The fine-tuning process ensures that the AE maintains its ability to generalize from the larger similar dataset while being sufficiently specialized to emphasize the distinct features of the smaller dataset. This refined AE is then utilized to generate the expanded synthesized dataset  $X'$ , depicted in the right portion of the Figure 1 (b), transitioning from the encoded representation  $Y'$  back to the image space using  $\phi^{-1}$ .

### 3.2 Feature Refinement: A Self-Attention Mechanism

In traditional language modeling, self-attention mechanisms are utilized to identify and weigh the relationships between different elements of a sequence, enabling the model to focus on the most relevant parts of the input for a given task Vaswani et al. [2017]. The row-wise self-attention mechanism typically used in these models may be sub-optimal for image data where spatial relationships are crucial. This is further discussed in Appendix E.

To enhance the capability of our Expansive Synthesis model in capturing spatial dependencies in image data, we propose a spatial multi-head self-attention mechanism, as illustrated in Fig. 6(b). This

mechanism entails dividing the encoded data into patches and positioning each flattened feature in its respective place within the stacked representation, without relying on positional encoding. The spatial self-attention is applied across all spatial dimensions, allowing the model to focus on significant features across the entire image. Detailed formulation and implementation of this mechanism can be found in Appendix E.

### 3.3 Expander Graph Mapping

The Expander Graph Mapping mechanism in our Expansive Synthesis(ES) model is designed to efficiently locate and interpolate features within the encoded space, generating new datapoints  $y_{\text{new}}$  in the synthesized dataset  $\mathbf{Y}'$ . Each datapoint  $y_i$  in the dataset  $Y \in \mathbb{R}^{n \times d}$  is associated to its own graph  $G_{y_i}^c = (V_{y_i}^c, E_{y_i}^c)$ . We have  $n/c$  such graphs, corresponding to the number of datapoints in each class, which is a subset of the distribution  $Y$ . For each datapoint  $y_i$ , we define  $G_{y_i}^c = (V_{y_i}^c, E_{y_i}^c)$  as its graph representation. We apply  $L$  self-attention heads  $SA.\text{Head}_j$  to produce feature maps  $f_{i,j}^c$ , where  $c$  denotes the class,  $i$  the datapoint index within the class ( $i \in \{1, \dots, n/c\}$ ), and  $j$  the feature index ( $j \in \{1, \dots, L\}$ ). The self-attention head calculates the importance of each feature relative to others, capturing dependencies within  $y_i$ . This is analytically expressed as,

$$f_{i,j}^c = SA.\text{Head}_j(y_i), \quad \forall j \in \{1, 2, \dots, L\}, \forall i \in \{1, \dots, n/c\}, \forall c \in \{1, \dots, C\}. \quad (2)$$

Following this, each  $f_{i,j}^c$  undergoes attention cropping, isolating and retaining the most relevant features from each feature map, extracting significant features by  $f_{i,j}^{c'} = \text{Att. Crop}(f_{i,j}^c)$ . During class-based training, we train each graph  $G_{y_i}^c \in \mathcal{G}^c$ , to maximize the spectral gap  $\lambda_2 - \lambda_1$  while preserving the spectral properties of the original data's graph Laplacian. The graph with the optimal spectral properties, denoted as  $\hat{G}^c$ , is selected as the codeword for that data class. The graph Laplacian  $\mathcal{L}$  for a graph  $G = (V, E)$  with  $|V| = L$  vertices is defined as  $\mathcal{L} = D - A$ , where  $D$  is a diagonal matrix with each diagonal element  $D_{ii}$  representing the degree of vertex  $i$ , and  $A$  is the adjacency matrix of the graph  $G$ . The eigenvalues of the Laplacian  $\mathcal{L}$  are  $\lambda_1, \lambda_2, \dots, \lambda_L$ , with  $\lambda_1 = 0$  for a connected graph. A larger gap  $\lambda_2 - \lambda_1$  indicates better connectivity Dey and Davis [2023]. The cropped features  $f_{i,j}^{c'}$  are placed into  $\mathbf{Y}'$  using convolutions  $\text{Conv}$ , guided by the selected expander graph  $\hat{G}^c = (V_{\hat{G}^c}, E_{\hat{G}^c})$ . This process constructs a new datapoint  $y'_{\text{new}}$  by integrating features with the expander graph, ensuring accurate feature placement:

$$y'_{\text{new}} = \sum_{j=1}^L \text{Conv}(f_{i,j}^{c'}, \hat{G}^c) \quad (3)$$

The convolution operation aligns  $f_{i,j}^{c'}$  with the vertices  $V_{\hat{G}^c}$  of  $\hat{G}^c$ , ensuring that each new vertex  $v' \in V_{y'_i}$  inherits the connectivity properties of  $G_{y_i}^c$  Dey and Davis [2023], Villani [2009]. The expander graph  $\hat{G}^c = (V_{\hat{G}^c}, E_{\hat{G}^c})$  maintains robust connectivity with a minimal number of edges. By embedding  $f_{i,j}^{c'}$  through  $\hat{G}^c$ ,  $G_{y'_i}^c$  preserves the spectral properties  $\lambda_{y_i,k} \approx \lambda_{y'_i,k}$  of  $G_{y_i}^c$ , maintaining structural robustness. The summation  $\sum_{j=1}^L \text{Conv}(f_{i,j}^{c'}, \hat{G}^c)$  ensures that  $y'_{\text{new}}$  retains the global structural properties of  $y_i$ , adhering to the expansion properties of  $\hat{G}^c$ . Leveraging the Expander Graph Mapping, our model smartly interpolates and locates features, ensuring the generation of new datapoints  $y'_{\text{new}}$  that are robust and structurally consistent with the original dataset. This method enhances the quality and diversity of the synthesized dataset  $\mathbf{Y}'$ , contributing to improved performance in downstream tasks. The driving intuition behind our proposed solution to dataset expansion lies in the projection of characteristic features  $Y$  in data at hand, and in their systematic, class-consistent, and distributionally-balanced packing  $Y'$  prior to reconstruction ( $X'$ ).

### 3.4 Loss Functions

The integrity of the generative ES flow in Fig. 6(b) is optimized using losses in guise of objectives, capturing the overall data reconstruction and classification loss as a global loss, together with a distributional consistency loss (Wasserstein distance) of the ES model, diversity loss and feature refinement loss for the local expansion optimization.

**Total Loss ( $\mathcal{L}_{\text{total}}$ ):** The overall objective of our model is guided by a weighted sum of multiple loss components, ensuring that the synthesized samples are diverse, persistent, and maintain a good cover of the distribution. The total loss is defined as:

$$\mathcal{L}_{\text{total}} = \alpha_0 \mathcal{L}_{re} + \alpha_1 \mathcal{L}_{ce} + \alpha_2 \mathcal{L}_{\mathcal{W}} + \alpha_3 \mathcal{L}_{cov} \quad (4)$$

where  $\alpha_0, \alpha_1, \alpha_2$ , and  $\alpha_3$  are hyperparameters that balance the different components of the loss function.

**Reconstruction Loss ( $\mathcal{L}_{re}$ ):** The autoencoder parametrization denoted by  $\phi$  and  $\theta$  for the encoder and decoder respectively follows the standard optimization loss between the input distribution and that of the output written as

$$\mathcal{L}_{re}(\phi, \theta; X) = \mathbb{E}_{Y \sim q_\phi(Y|X)} [-\log p_\theta(X|Y)] + \text{KL}[q_\phi(Y|X) || p(Y)], \quad (5)$$

where the first term is the expected negative log-likelihood, and the second term is the Kullback-Leibler divergence between the encoded distribution  $q_\phi(Y|X)$  and a prior distribution  $p(Y)$  Goodfellow et al. [2014]. To selectively exploit the most relevant features and further refine the intrinsic linear evolution of the nonlinear dynamics, we precede the the expander graph mapping and multi-head spatial self-attention transformation on  $Y$  to yield  $Y' \in \mathbb{R}^{n' \times d}$  Vaswani et al. [2017]. In the expansion phase,  $Y'$  is crafted to be of higher dimension ( $n'$ ) while still reflecting the original dataset's distribution. This process is guided by the minimization of the Wasserstein distance [Vaserstein, 1969]  $\mathcal{W}(Y, Y')$ , ensuring that the expanded data  $Y'$  maintains the distributional integrity of  $Y$ .

**Distributional Consistency ( $\mathcal{L}_{\mathcal{W}}$ ):** The concept of Wasserstein distance arises as a specialized form of the Optimal Transport Loss Villani [2009], where it specifically measures the cost to align the distribution of the encoded data  $Y$  with that of the expanded representation  $Y'$ . The Wasserstein distance [Vaserstein, 1969], therefore, quantifies the minimal "effort" required to morph the distribution  $p_Y$  into  $p_{Y'}$ , making it a natural measure for the effectiveness of dataset expansion processes Roheda et al. [2023]. The Wasserstein distance can be expressed as:

$$\mathcal{L}_{\mathcal{W}}(p_Y, p_{Y'}) = \min_{\pi \in \Pi(p_Y, p_{Y'})} \iint c(Y, Y') \pi(p_Y, p_{Y'}) dY dY' \quad (6)$$

In this formulation,  $\pi$  corresponds to the optimal transport plan that associates the distributions  $p(Y)$  and  $p(Y')$ . By minimizing the Wasserstein distance  $\mathcal{L}_{\mathcal{W}}$ , we aim to ensure that the expanded dataset  $Y'$  not only statistically resembles the original dataset  $Y$  but also preserves its geometric and topological properties, crucial for maintaining the fidelity of the expanded data for subsequent learning tasks that depend on the intricate relationships within the data's manifold structure Villani [2009]. The expanded representation  $Y'$  is subsequently mapped back into the high-dimensional image space using the same decoder function  $\phi^{-1}$  that was initially used for encoding. This results in the expanded dataset  $X'$ , where  $X' \in \mathbb{R}^{n' \times D}$ . The utilization of the same autoencoder for both encoding and decoding stages ensures that the expanded data  $X'$  is a plausible output of the autoencoder, retaining the structure and distributional properties of the original dataset. A classifier  $f_c$  is then trained on the reconstructed expanded dataset  $X'$ , which is equipped to predict the output labels  $\hat{y}$  as if it were trained on the original dataset  $X$ . This process allows the classifier to benefit from the distilled information within  $X'$ , enabling efficient training with significantly reduced computational resources.

**Classification Loss ( $\mathcal{L}_{ce}$ ):** Central to our model is the classification loss, which serves as a form of implicit feedback information. It evaluates the discrepancy between the predicted labels obtained from the classifier and the true labels, guiding the latent representation towards maintaining label consistency. Crucially, this process involves both the original and synthesized expanded images ( $X$  and  $X'$ ), which are merged and passed through the classifier to ensure comprehensive learning. The Cross-Entropy (CE) loss metric is utilized for this purpose:

$$\mathcal{L}_{ce}(f_c, \tilde{X}, y) = - \sum_i y_i \log(f_c(\tilde{X}_i)) \quad (7)$$

Here,  $f_c$  represents the classifier function,  $\tilde{X}$  is the combined set of original and reconstructed data,  $y$  is the vector of true labels, and  $\tilde{X}_i$  refers to the  $i$ -th data instance in the merged dataset Goodfellow et al. [2014]. This loss component is instrumental in ensuring that the expanded dataset encapsulates

not only the structural attributes of the original data but also its label characteristics, thus preserving essential discriminative features and preventing the dilution of categorical information during the dataset expansion process.

The Koopcon model leverages the computational efficiency of linear dynamics in the encoded space and the cognitive economy of the brain’s predictive coding strategy Friston and Kiebel [2009]. It presents a significant advancement in creating data-efficient learning strategies, allowing for scalable training on extensive datasets while maintaining performance parity with models trained on the full dataset.

**Expansion Diversity Loss ( $\mathcal{L}_{cov}$ ):** To foster a more diverse and representative expanded dataset, we introduce a covariance loss term into the overall loss function. This term serves as a regularizer, promoting the capture of distinct features within the latent representations  $Y$ . When examining the encoded versions of all  $Y_i$ s against the encoded version of representative  $Y'_i$ s, the necessity for such a loss term becomes apparent. In scenarios without the covariance loss, the representatives tend to cluster together, leading to a less diversified representation. Conversely, the inclusion of covariance loss encourages a more scattered distribution of representatives  $Y'_i$ s, thereby enhancing the diversity within the dataset. The mathematical definition of Covariance Loss is given by:

$$\mathcal{L}_{cov}(Y') = \|\text{Cov}(Y') - I\|_F^2, \quad (8)$$

where  $\text{Cov}(Y')$  denotes the covariance matrix of the latent representation  $Y'$ ,  $I$  is the identity matrix, and  $\|\cdot\|_F$  represents the Frobenius norm. By minimizing  $\mathcal{L}_{cov}$ , the model is encouraged to produce features that are uncorrelated, thereby increasing the informativeness and variability of the synthesized samples. This discourages feature redundancy, which is instrumental in avoiding overfitting and improving the model’s ability to generalize from synthesized representatives to unseen data. Thus, the Covariance Loss plays a pivotal role in ensuring that the expanded dataset is not only a compressed version of the original data but also a functionally diverse subset that retains the original’s rich feature set Friston and Kiebel [2009], Vaserstein [1969].

---

#### Algorithm 1 Expansive Syn. Train Algorithm

---

```

1: Given:
2:  $X \in \mathbb{R}^{n \times D}$ , original dataset with  $n$  samples
3:  $\phi$ : Encoder mapping  $\mathbb{R}^D \rightarrow \mathbb{R}^d$ 
4:  $\phi^{-1}$ : Decoder mapping  $\mathbb{R}^d \rightarrow \mathbb{R}^D$ 
5: MHSSA: Multi-head Spatial Self-attention
6: EGM: Expander Graph Mapping
7:  $n'$ : Target number of synthesized samples
8:  $\alpha_0, \alpha_1, \alpha_2, \alpha_3$ : Weights for loss components
9: N: Number of training epochs
10: M: Number of classes of data
11: Initialize: Parameters of AE ( $\phi, \phi^{-1}$ ), Classifier  $f_c$ 
12: for epoch = 1 to N do
13:   for class = 1 to M do
14:      $Y \leftarrow \phi(X)$ 
15:      $Y_{SA} \leftarrow \text{MHSSA}(Y)$ 
16:      $Y' \leftarrow \text{EGM}(Y_{SA})$ 
17:      $X' \leftarrow \phi^{-1}(Y')$ 
18:      $L_{re} \leftarrow \|X' - X\|^2$ 
19:      $\hat{Y} \leftarrow f_c(X \oplus X')$ , ( $\oplus$ : concatenation)
20:      $L_{ce} \leftarrow -\sum_i y_i \cdot \log(\hat{Y})$ , ( $y_i$ : true labels)
21:      $\mathcal{L}_{\mathcal{W}} \leftarrow \mathcal{W}(Y, Y')$ , ( $\mathcal{W}$ : Wasserstein Distance)
22:      $\mathcal{L}_{cov}(Y') \leftarrow \|\text{Cov}(Y') - I\|_F^2$ 
23:      $L_{total} \leftarrow \alpha_0 L_{re} + \alpha_1 L_{ce} + \alpha_2 \mathcal{L}_{\mathcal{W}} + \alpha_3 \mathcal{L}_{cov}$ 
24:     Update Parameters

```

---



---

#### Algorithm 2 Expansive Syn. Test Algorithm

---

```

1: Given:
2:  $X_{\text{train}}, X_{\text{test}}$ , real train and test data
3:  $\phi$ : Encoder mapping  $\mathbb{R}^D \rightarrow \mathbb{R}^d$ 
4:  $\phi^{-1}$ : Decoder mapping  $\mathbb{R}^d \rightarrow \mathbb{R}^D$ 
5: MHSSA: Multi-head Spatial Self-attention
6: EGM: Expander Graph Mapping
7: Classifiers  $f_c$ 
8: N: Number of training epochs
9: M: Number of classes
10: Initialize:
11: Load trained parameters for AE ( $\phi, \phi^{-1}$ )
12: for epoch = 1 to N do
13:   for class = 1 to M do
14:      $Y \leftarrow \phi(X_{\text{train}})$ 
15:      $Y_{SA} \leftarrow \text{MHSSA}(Y)$ 
16:      $Y' \leftarrow \text{EGM}(Y_{SA})$ 
17:      $X' \leftarrow \phi^{-1}(Y')$ 
18:      $f_c^{\text{synth}}$ : Train classifier  $f_c$  on  $X'$ 
19:      $f_c^{\text{real}}$ : Train classifier  $f_c$  on  $X_{\text{train}}$ 
20: Evaluate: Test  $f_c^{\text{synth}}$  and  $f_c^{\text{real}}$  on  $X_{\text{test}}$ 
21: Compare Performance:
22: Calculate and report accuracy for both classifiers

```

---

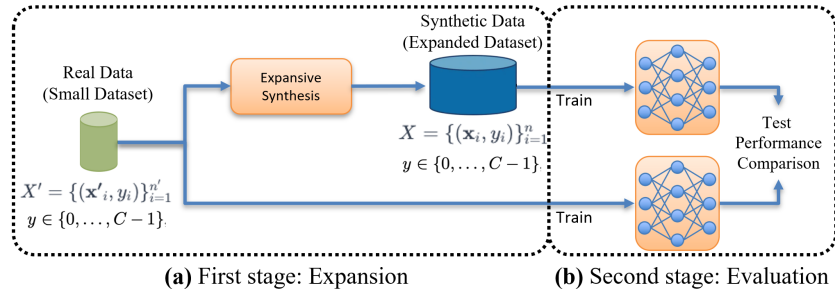


Figure 3: Stages of Implementation and evaluation of an expansion model

## 4 Experiments and Results

### 4.1 Stages of Implementation

The stages of implementation are illustrated in Figure 2, which outlines the two-phase process of dataset expansion and subsequent evaluation.

**First Stage (Expansion):** We begin with a small dataset  $X$ , consisting of pairs  $(x_i, y_i)$  where  $x_i$  represents the input data and  $y_i$  the corresponding labels. The dataset has  $n$  such pairs, and labels range over  $C$  different classes, from 0 to  $C - 1$ . This small dataset  $X$  undergoes an expansion process to produce a much larger, synthesized dataset  $X'$ . This expanded dataset contains pairs  $(x'_i, y_i)$ , where  $x'_i$  are the synthesized features (expanded representations) and  $y_i$  are the corresponding labels. There are  $n'$  pairs in  $X'$ , and it maintains the same range of labels as the original dataset.

**Second Stage (Evaluation):** The synthesized dataset  $X'$  is then used to train a classifier. The classifier learns to predict labels based on the expanded feature set provided by  $X'$ . In parallel, we train the same type of classifier on the small dataset  $X$ . This dataset is augmented in the classic way to have the same number of examples  $n'$  as the synthesized dataset to make a fair comparison. After both classifiers are trained, their performance is evaluated on a test set. The goal is to demonstrate that the classifier trained on the synthesized dataset  $X'$  performs better than the classifier trained on the augmented real dataset  $X$ , despite  $X'$  being significantly smaller in size.

The underlying hypothesis is that if the synthesized dataset  $X'$  is a good expansion of  $X$ , then the classifier trained on  $X'$  should generalize almost as well as the classifier trained on  $X$  when evaluated on unseen data. This would show that  $X'$  successfully captures the core information from the larger dataset  $X$ , enabling effective training with much less data.

### 4.2 Results and Comparisons

Table 1: Classification accuracy results (%) initiated with 10 images per class (Img/Cls) post expansion for our expansive synthesis model with different settings on different datasets. Acronyms: RwA (Row-wise Attention), SA (Self-Attention), SC (Skip Connections), MHSA (Multi-Head Self-Attention), EGM (Expander Graph Mapping).

	Dataset / Exp. Setting	Original data	Expanded data				
		-	RwA	SA	SA + SC	MHSA + SC	MHSA + SC + EGM
Initiated with 10 Img/Cls (E.R. = 10)	MNIST	52.3	63.2	65.1	68.6	69.1	<b>69.5</b>
	CIFAR-10	41.5	52.1	54.2	58.7	60.1	<b>63.1</b>
	CIFAR-100	30.1	42.3	44.7	49	52.3	<b>55.1</b>

This section presents the experimental results of our Expansive Synthesis model, demonstrating its effectiveness in generating large-scale, high-fidelity datasets from minimal samples. We evaluate classifiers trained on these synthesized datasets against those trained on original and classically augmented datasets. Table 1 compares classification accuracies across MNIST [Deng, 2012], CIFAR-10, and CIFAR-100 [Krizhevsky and Hinton, 2009]. Classifiers trained on 10 original images achieve the lowest accuracies, highlighting the limitations of minimal data. Introducing expansive synthesis with row-wise self-attention significantly improves accuracy across all datasets, with an



Table 2: Classification accuracy results (%) initiated by 100 Img/Cls post expansion for our expansive synthesis model with different settings on different datasets

Initiated with 100 Img/Cls (E.R. = 10)	Dataset / Exp. Setting	Original data	Expanded data				
		-	RwA	SA	SA + SC	MHSA + SC	MHSA + SC + EGM
	MNIST	64.9	74.7	76.1	80.4	83.1	<b>84.1</b>
	CIFAR-10	52	62.9	64.7	69.8	73.9	<b>74.4</b>
	CIFAR-100	38.3	51.2	54.2	59.1	63.5	<b>63.9</b>

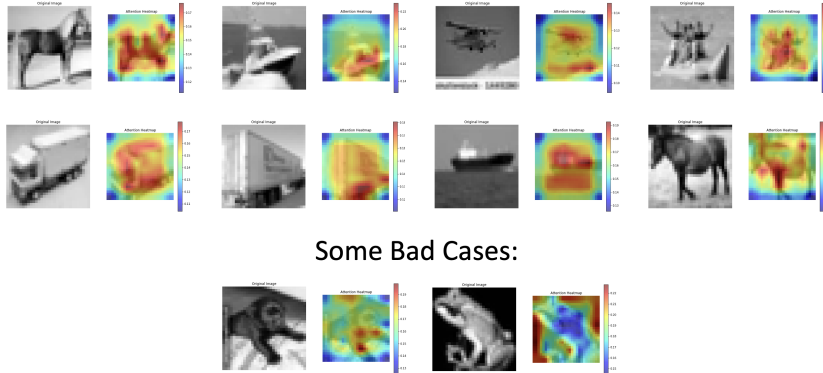


Figure 4: Heat-map results of the Multi-head Self-attention module in the encoded space

average 20% improvement over the baseline. Spatial attention further enhances performance by 6% on average, capturing spatial dependencies more effectively. Adding skip connections to spatial attention yields an additional 8% improvement, preserving essential information from the encoded data. Multi-head spatial self-attention boosts results by 4%, capturing diverse discriminative features in parallel. Finally, incorporating Expander Graph Mapping (EGM) achieves the best results, with a 6% enhancement over the previous configuration, leading to superior feature representation. The ablation study shows that each module incrementally improves performance, culminating in a model that generates high-fidelity datasets from minimal samples. This is particularly evident with the addition of multi-head self-attention and EGM, which optimize feature representation.

Table 3, compares classification accuracy for models initialized with either 10 or 100 images per class across MNIST, CIFAR-10, and CIFAR-100. The expansive synthesis model consistently outperforms traditional augmentation. For example, on MNIST, accuracy improves from 52.3% to 54.7% with 10 images per class and from 64.9% to 66.8% with 100 images per class. Similar improvements are observed for CIFAR-10 and CIFAR-100. These findings highlight the effectiveness of our model in enhancing dataset quality and classifier performance.

Table 3: Comparison of classification accuracy (%) for models initiated with 10 and 100 images per class (Img/Cls) across different datasets: MNIST, CIFAR-10, and CIFAR-100. The table compares the performance of classifiers trained on original data, classically augmented data, and data expanded using our expansive synthesis method, all with the same Expansion Ratio (ER = 10).

	Initiated with 10 Img/Cls (E. R. = 10)			Initiated with 100 Img/Cls (E. R. = 10)		
	Original data	Classically Augmented	MHSA + SC + EGM	Original data	Classically Augmented	MHSA + SC + EGM
MNIST	52.3	54.7	<b>69.5</b>	64.9	66.8	<b>84.1</b>
CIFAR-10	41.5	46.7	<b>63.1</b>	52	57.4	<b>74.4</b>
CIFAR-100	30.1	32.8	<b>55.1</b>	38.3	41.5	<b>63.9</b>

## 5 Conclusion and Future Works

In this paper, we introduced the Expansive Synthesis model, which generates large-scale, high-fidelity datasets from minimal samples. Utilizing the Koopman feature space within an autoencoder (AE) architecture, our model effectively transforms non-linear latent space features into a linear space.

The multi-head spatial self-attention mechanism improves feature extraction by capturing different discriminative features, enhancing the detail and accuracy of the synthesized data. Following this, the expander graph mappings maintain the connectivity and relevance of different features during expansion, ensuring robust feature representation. To preserve intrinsic data distributions, optimal transport is employed, while a diversity loss based on covariance loss ensures a diverse set of synthesized data points. An ablation study highlights the importance and improvement contributed by each module. Experimental results across different complex low-resolution datasets show that classifiers trained on our synthesized datasets achieve significantly better performance compared to those trained on minimal samples and outperform traditional data augmentation techniques. Future work could integrate Expansive Synthesis with diffusion models for enhanced data quality and diversity. Additionally, applying domain adaptation techniques will allow customization for real-time applications in fields like autonomous driving and personalized healthcare, ensuring high performance and adaptability.

## References

- Anonymous. Koopcon: A new approach towards smarter and less complex learning. *arXiv preprint arXiv:submit/5605804*, 2024.
- Nitesh V Chawla, Kevin W Bowyer, Lawrence O Hall, and W Philip Kegelmeyer. Smote: Synthetic minority over-sampling technique. *Journal of Artificial Intelligence Research*, 16:321–357, 2002.
- Ekin D. Cubuk, Barret Zoph, Dandelion Mane, Vijay Vasudevan, and Quoc V. Le. Autoaugment: Learning augmentation strategies from data. In *Proceedings of the IEEE/CVF Conference on Computer Vision and Pattern Recognition (CVPR)*, 2019.
- Li Deng. The mnist database of handwritten digit images for machine learning research [best of the web]. *IEEE Signal Processing Magazine*, 29(6):141–142, 2012.
- Sourya Dey and Eric William Davis. Dkoopman: A deep learning software package for koopman theory. In *Learning for Dynamics and Control Conference. PMLR*, 2023.
- Michael A. Forbes and Venkatesan Guruswami. Dimension expanders via rank condensers. *CoRR*, abs/1411.7455, 2014. URL <http://arxiv.org/abs/1411.7455>.
- Karl Friston and Stefan Kiebel. Predictive coding under the free-energy principle. *Philosophical transactions of the Royal Society B: Biological sciences*, 364(1521):1211–1221, 2009.
- Leon A. Gatys, Alexander S. Ecker, and Matthias Bethge. A neural algorithm of artistic style. *arXiv preprint arXiv:1508.06576*, 2015.
- Ian J. Goodfellow, Jean Pouget-Abadie, Mehdi Mirza, Bing Xu, David Warde-Farley, Sherjil Ozair, Aaron Courville, and Yoshua Bengio. Generative adversarial nets. In *Advances in Neural Information Processing Systems 27 (NIPS 2014)*, 2014.
- Kaiming He, Xiangyu Zhang, Shaoqing Ren, and Jian Sun. Deep residual learning for image recognition. In *Proceedings of the IEEE Conference on Computer Vision and Pattern Recognition*, 2016.
- Justin Johnson, Alexandre Alahi, and Li Fei-Fei. Perceptual losses for real-time style transfer and super-resolution. In *Proceedings of the European Conference on Computer Vision (ECCV)*, 2016.
- Bernard O. Koopman. Hamiltonian systems and transformation in hilbert space. *Proceedings of the National Academy of Sciences*, 17(5):315–318, 1931.
- Alex Krizhevsky and Geoffrey Hinton. Learning multiple layers of features from tiny images. Technical report, Technical Report, 2009.
- Alex Krizhevsky, Ilya Sutskever, and Geoffrey E Hinton. Imagenet classification with deep convolutional neural networks. In *Advances in Neural Information Processing Systems 25 (NIPS 2012)*, 2012.
- Gregory A Margulis. Explicit constructions of expanding graphs. *Problemy Peredachi Informatsii*, 9(4):71–80, 1973.

- Alec Radford, Luke Metz, and Soumith Chintala. Unsupervised representation learning with deep convolutional generative adversarial networks. *arXiv preprint arXiv:1511.06434*, 2015.
- Siddharth Roheda, Ashkan Panahi, and Hamid Krim. Fast optimal transport for latent domain adaptation. In *2023 IEEE International Conference on Image Processing (ICIP)*, pages 1810–1814. IEEE, 2023.
- Leonid Nisonovich Vaserstein. Markov processes over denumerable products of spaces, describing large systems of automata. *Problemy Peredachi Informatsii*, 5(3):64–72, 1969.
- Ashish Vaswani, Noam Shazeer, Niki Parmar, Jakob Uszkoreit, Llion Jones, Aidan N Gomez, Łukasz Kaiser, and Illia Polosukhin. Attention is all you need. In *Advances in Neural Information Processing Systems 30 (NIPS 2017)*, 2017.
- Cédric Villani. *Optimal transport: old and new*, volume 338. Springer, 2009.
- Jun-Yan Zhu, Taesung Park, Phillip Isola, and Alexei A. Efros. Unpaired image-to-image translation using cycle-consistent adversarial networks. In *Proceedings of the IEEE International Conference on Computer Vision (ICCV)*, 2017.

## Appendix / supplemental material

In this section, we provide an overview of the foundational theories that underpin our work. We begin with an introduction to Koopman operator theory, which offers a linear perspective on nonlinear dynamical systems. This is followed by a discussion on the integration of deep learning techniques to approximate Koopman operators, enhancing the practical applicability of the theory. Finally, we delve into the role of optimal transport theory in ensuring the fidelity and efficiency of dataset expansion, highlighting recent advancements that inform our approach.

### A Koopman Operator Theory

Koopman operator theory offers a rich and elegant framework for analyzing nonlinear dynamical systems by transforming them into a linear context. First proposed by Koopman in Koopman [1931], the theory facilitates the study of complex systems using linear operators on function spaces, regardless of the nonlinearity in the state space.

**Theorem 1 (Koopman Operator Linearity)** *Given a nonlinear dynamical system with state evolution defined by  $\bar{x}_{t+1} = f(\bar{x}_t)$ , where  $\bar{x}_t$  (the system state at time  $t$ )  $\in \mathcal{M} \subseteq \mathbb{R}^n$  and  $f : \mathcal{M} \rightarrow \mathcal{M}$ , the Koopman operator  $\mathcal{K} : \mathcal{H} \rightarrow \mathcal{H}$  acts linearly on observable functions  $g : \mathcal{M} \rightarrow \mathbb{R}$  in the Hilbert space  $\mathcal{H}$ , such that:*

$$(\mathcal{K}g)(x_t) = g(f(x_t)) = g(x_{t+1}) \quad (9)$$

The theorem emphasizes that the Koopman operator advances observables  $g$  linearly in time according to the system’s dynamics. The eigenfunctions  $\psi$  of the Koopman operator satisfy the linear eigenvalue equation  $\mathcal{K}\psi(x) = \lambda\psi(x)$ , with  $\lambda$  as the eigenvalue, indicating a scaled or rotated evolution of the eigenfunction, with its structure preserved over time.

### B Deep Koopman Operator

Expanding upon Koopman’s theory, recent advancements in deep learning Dey and Davis [2023] have facilitated the approximation of the Koopman operator using neural networks, allowing for practical applications in a variety of complex systems.

**Theorem 2 (Deep Koopman Learning)** *Observations  $X = [x_1, x_2, \dots, x_t]$  and their time-evolved states  $X' = [x_2, x_3, \dots, x_{t+1}]$  of a dynamical system can be utilized to learn a neural network approximation of the Koopman eigenfunctions  $\phi(\cdot)$  and the linear dynamics embodied by a matrix  $T$  in state space  $\mathcal{Y}$ , by minimizing the loss function:*

$$\min_{\phi, T} \|\hat{X}' - X'\|^2, \quad (10)$$

where  $\hat{X}'$  are the predicted future states generated by the learned dynamics.

We adopt an autoencoder to capture the K-eigenfunction  $\phi(\cdot)$  and the linear operations inside the encoded space. The encoder maps the input data into a latent space representing the Koopman observables, and the decoder reconstructs the state space from these observables. The linear evolution in the latent space is governed by the learned matrix  $T$ , analogous to the Koopman matrix  $K$ , facilitating the prediction of future system states. As described in Dey and Davis [2023], DLKoopman provides a bridge between non-linear dynamics and linear predictive models.

## C Notations

For clarity and consistency throughout this paper, the following notations are adopted, where capital boldface lower case letters respectively denote matrices and vectors, and subscripts denote vector elements while superscripts indicate an alternative copy in a sequence or a transformation.

- $X$ : The original high-dimensional and large-scale dataset, where each element  $x_i$  represents an individual data point with associated features.
- $Y$ : The latent representation of  $X$  obtained after encoding through the autoencoder’s encoder network  $\phi$ .
- $X'$ : The Expanded dataset synthesized from  $X$ , which is smaller in size but designed to retain the essential information of the original dataset.
- $Y'$ : The Expanded latent representation of  $Y$ , which is the result of applying the Expansion process within the latent space.
- $\phi$ : The encoder part of the autoencoder that maps the input data  $X$  to its latent representation  $Y$ .
- $\phi^{-1}$ : The decoder part of the autoencoder that maps the latent representation  $Y$  back to the reconstructed data  $\hat{X}$  or  $X'$ .
- $f_c$ : The classifier function trained on the reconstructed Expanded dataset  $X'$ .
- $\mathcal{W}$ : The Wasserstein distance used to measure distributional discrepancies in the Expansion process.

## D Optimal Transport

Data expansion may be abstractly interpreted as a generalized smart augmentation in that a number of data entities (e.g., images) are expanded, while methodically preserving all associated characteristic features. In so doing, we seek to quantitatively track this task by comparing the resulting distributions to that prior, using a measure derived from optimal transport theory. This approach draws upon recent advancements (like in Villani [2009] and Roheda et al. [2023]), integrating principles of optimal transport to enhance the fidelity and efficiency of dataset expansion, thereby preserving essential information while achieving significant reductions in data volume.

Integral to our model is the minimization of the cost  $c$  for transforming the encoded latent representation of original data with a probability density function  $p(Y)$  to closely match that of expanded version of data  $p(Y')$ . This is articulated through the Optimal Transport Loss:

$$\mathcal{L}_{O.T.} = \min_{\pi \in \Pi(p(Y), p(Y'))} \mathbb{E}_{(Y, Y') \sim \pi} [c(Y, Y')] \quad (11)$$

Here,  $\pi$  represents a coupling between the distributions  $p(Y)$  and  $p(Y')$ , with  $c(Y, Y')$  denoting the dissimilarity measure between  $Y$  and  $Y'$ .

## E Self-Attention Mechanisms in Expansive Synthesis

In traditional language models, self-attention mechanisms are utilized to identify and weigh the relationships between different elements of a sequence, enabling the model to focus on the most relevant parts of the input for a given task Vaswani et al. [2017]. The row-wise self-attention

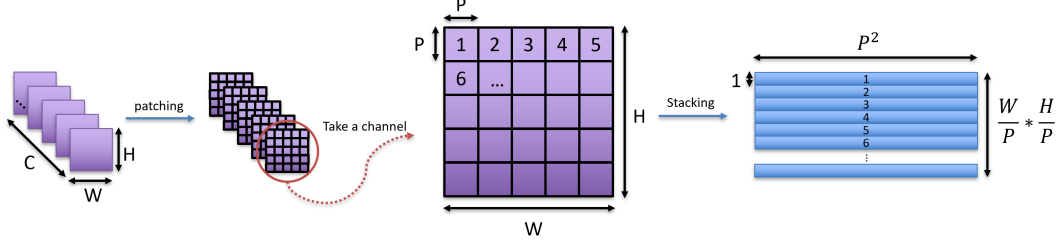


Figure 5: Row-wise attention's patching and stacking method in Expansive Synthesis

mechanism typically used in these models operates by dividing the input data into smaller patches and applying attention across each row of these patches. This approach is effective for capturing dependencies in sequential data but may not be optimal for image data where spatial relationships are crucial.

### E.1 Row-Wise Self-Attention Mechanism

In our implementation, as depicted in Figure 5, the encoded data  $\mathbf{Y} \in \mathbb{R}^{n \times C \times H \times W}$  is first divided into patches of size  $P \times P$ . Each channel is taken separately, and the patches are stacked, resulting in a sequence of patches  $\mathbf{Y}_{\text{patch}} \in \mathbb{R}^{n \times C \times (H/P) \times (W/P) \times P^2}$ . The row-wise self-attention mechanism is then applied, attending to each row of the stacked patches. This mechanism can be mathematically formulated as:

$$\text{Attention}(Q, K, V) = \text{softmax} \left( \frac{QK^T}{\sqrt{d_k}} \right) V \quad (12)$$

where  $Q$ ,  $K$ , and  $V$  are the query, key, and value matrices derived from the input patches, and  $d_k$  is the dimension of the key vectors Vaswani et al. [2017], Radford et al. [2015].

### E.2 Proposed Spatial Multi-Head Self-Attention Mechanism

To enhance the capability of our Expansive Synthesis model in capturing spatial dependencies in image data, we propose a spatial multi-head self-attention mechanism. As illustrated in Figure 6, this mechanism involves dividing the encoded data into patches and positioning each flattened feature in its respective place within the stacked representation, without relying on positional encoding. The spatial self-attention is applied across all spatial dimensions, allowing the model to focus on significant features across the entire image.

The spatial self-attention mechanism is defined as follows:

1. Patching: The encoded data is divided into patches of size  $P \times P$ :

$$\mathbf{Y}_{\text{patch}} \in \mathbb{R}^{n \times C \times (H/P) \times (W/P) \times P^2} \quad (13)$$

2. Flattening and Positioning: Each patch is flattened, and the features are positioned in their respective places within the stacked representation. This results in a 3D tensor  $\mathbf{Y}_{\text{stacked}} \in \mathbb{R}^{n \times C \times (H/P) \times (W/P) \times P^2}$ , maintaining the spatial structure of the image data.

3. Multi-Head Attention: Apply multi-head attention to capture diverse spatial features:

$$\text{MultiHead}(Q, K, V) = \text{Concat}(\text{head}_1, \dots, \text{head}_h)W^O \quad (14)$$

where each head is computed as:

$$\text{head}_i = \text{Attention}(QW_i^Q, KW_i^K, VW_i^V) \quad (15)$$

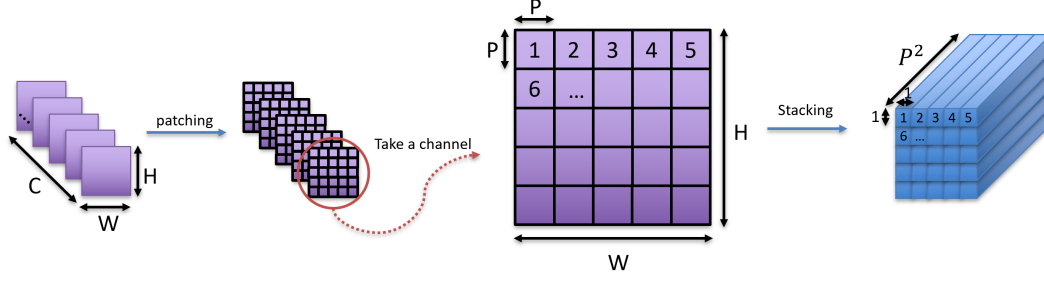


Figure 6: Spatial Multi-Head Self-Attention’s patching and stacking approach in Expansive Synthesis

with  $W_i^Q$ ,  $W_i^K$ ,  $W_i^V$  being the projection matrices for the  $i$ -th head [Vaswani et al., 2017, He et al., 2016].

4. Aggregation and Transformation: Aggregate the attended features and transform them back to the original spatial dimensions:

$$\mathbf{Y}' = \text{Reshape}(\text{MultiHead}(Q, K, V)) \quad (16)$$

5. Loss Function: The loss function for training the self-attention mechanism includes a Wasserstein distance term and a covariance loss term to ensure the expanded feature maps  $\mathbf{Y}'$  are similar to the original encoded data  $\mathbf{Y}$ :

$$\mathcal{L} = \min(W(\mathbf{Y}, \mathbf{Y}') + \mathcal{L}_{\text{cov}}(\mathbf{Y}')) \quad (17)$$

By incorporating this spatial multi-head self-attention mechanism, our Expansive Synthesis model effectively identifies and enhances the most significant features in the encoded space, enabling the generation of a more detailed and enriched synthesized dataset  $\mathbf{X}'$ . This approach not only preserves the essential characteristics of the original data but also amplifies critical features, contributing to more robust performance in downstream classification tasks.